The Astrophysical Journal, 749:116 (8pp), 2012 April 20 doi:10.1088/0004-637X/749/2/116

SPATIALLY RESOLVED [Fe II] 1.64 μm EMISSION IN NGC 5135: CLUES FOR UNDERSTANDING THE ORIGIN OF THE HARD X-RAYS IN LUMINOUS INFRARED GALAXIES

L. Colina[1], M. Pereira-Santaella[1], A. Alonso-Herrero[1,3], A. G. Bedregal[2], and S. Arribas[1]
[1] Astrophysics Department, Center for Astrobiology (CSIC-INTA), Torrejon de Ardoz, 28850 Madrid, Spain; colina@cab.inta-csic.es
[2] Department of Astronomy, University of Minnesota, 116 Church Street S.E., Minneapolis, MN 55455, USA
Received 2011 July 11; accepted 2012 February 6; published 2012 March 29

ABSTRACT

Spatially resolved near-IR and X-ray imaging of the central region of the luminous infrared galaxy (LIRG) NGC 5135 is presented. The kinematical signatures of strong outflows are detected in the [Fe II] 1.64 μm emission line in a compact region at 0.9 kpc from the nucleus. The derived mechanical energy release is consistent with a supernova rate of 0.05–0.1 yr^{-1}. The apex of the outflowing gas spatially coincides with the strongest [Fe II] emission peak and with the dominant component of the extranuclear hard X-ray emission. All these features provide evidence for a plausible direct physical link between supernova-driven outflows and the hard X-ray emitting gas in an LIRG. This result is consistent with model predictions of starbursts concentrated in small volumes and with high thermalization efficiencies. A single high-mass X-ray binary (HMXB) as the major source of the hard X-ray emission, although not favored, cannot be ruled out. Outside the active galactic nucleus, the hard X-ray emission in NGC 5135 appears to be dominated by the hot interstellar medium produced by supernova explosions in a compact star-forming region, and not by the emission due to HMXBs. If this scenario is common to (ultra)luminous infrared galaxies, the hard X-rays would only trace the most compact ($\leqslant$100 pc) regions with high supernova and star formation densities, therefore a lower limit to their integrated star formation. The star formation rate derived in NGC 5135 based on its hard X-ray luminosity is a factor of two and four lower than the values obtained from the 24 μm and soft X-ray luminosities, respectively.

Key words: galaxies: individual (NGC 5135) – galaxies: starburst – infrared: galaxies – X-rays: galaxies

Online-only material: color figures

1. INTRODUCTION

Luminous infrared galaxies (LIRGs) with infrared (8–1000 μm) luminosities (L_{IR}) of 10^{11}–10^{12} $L_{\odot}$ are powered mainly by star formation with some contribution from an active galactic nucleus (AGN) in a fraction of them (Genzel et al. 1998; Nardini et al. 2008; Alonso-Herrero et al. 2012). Aside from the contribution by the compact AGN, if present, the X-ray luminosity in LIRGs is produced by the star formation. As such, correlations between the star formation rate (SFR), independently derived from the IR luminosity, and the X-ray luminosity are expected. These correlations for both soft (0.5–2 keV) and hard (2–10 keV) X-rays have recently been obtained in a sample of LIRGs (Pereira-Santaella et al. 2011, and references therein). These galaxies follow the same linear correlations found for normal star-forming galaxies within a factor of two scatter. The physical origin of the extension of these correlations to luminous and compact starbursts with SFR of up to 100 $M_{\odot}$ yr^{-1} is not fully clear. While the soft X-ray emission is assumed to be dominated by the diffuse, extended (kpc size) emission of a hot (10^6–10^7 K) starburst-driven gas (Strickland et al. 2002; Ranalli et al. 2003; McDowell et al. 2003), the hard X-rays are assumed to be predominantly due to the collective emission of luminous high-mass X-ray binaries (HMXBs) and therefore associated with unresolved sources (Grimm et al. 2003; Persic 2004; Strickland & Heckman 2007). However, high angular X-ray imaging of M82 (Strickland & Heckman 2007) has shown the presence of a diffuse component contributing about one-third of the 3–10 keV luminosity. Moreover, non-AGN ultraluminous infrared galaxies (ULIRGs) and high-luminosity LIRGs show in their integrated spectrum strong Fe XXV at 6.7 keV, which is not produced by HMXBs but rather likely due to a high-temperature ($T \sim 10^8$ K) thermal gas (Iwasawa et al. 2009). These authors conclude that unlike for local star-forming galaxies, HMXBs are not the primary source of the hard X-ray band emission seen in non-AGN luminous LIRGs ($L_{IR} \geqslant 5 \times 10^{11}$ $L_{\odot}$), suggesting that a transition in the nature of the dominant hard X-ray source in LIRGs occurs somewhere in the range log L_{IR} =11.0–11.73 $L_{\odot}$ (Iwasawa et al. 2011). These results seem to give support to recent starburst-driven wind models (Strickland & Heckman 2009) where a very hot plasma (10^7 K $< T < 10^8$ K) produced by the thermalization of the mechanic energy released by supernova explosions in compact starbursts would be a major contributor to the hard X-ray emission. A contribution to the Fe XXV emission at 6.7 keV in (U)LIRGs could also come from heavily obscured AGNs. However, *XMM* surveys of Seyferts have shown that the 6.7 keV Fe XXV line is detected in only a small fraction (3 out of 26) of the surveyed galaxies (Nandra et al. 2007). In addition, recent studies of the nearby edge-on starburst galaxy NGC 253 have demonstrated that the Fe XXV 6.7 keV emission is not dominated by the obscured AGN but by an extended hot gas emission outside the nucleus. The origin of this emission is consistent with the presence of supernovae and supernovae remnants, with a minor contribution from HMXBs and cataclysmic variables (Mitsuishi et al. 2011).

In order to investigate the different scenarios and physical origin of the hard X-ray emission, i.e., extended hot plasma gas associated with supernova versus point sources (HMXBs, AGNs), spatially resolved imaging of supernovae tracers (e.g., radio or near-IR [Fe II] 1.64 μm emission) and of the X-ray emission are needed. So far, such studies have been carried

[3] Also at Instituto de Física de Cantabria, CSIC-UC, 39005 Santander, Spain.

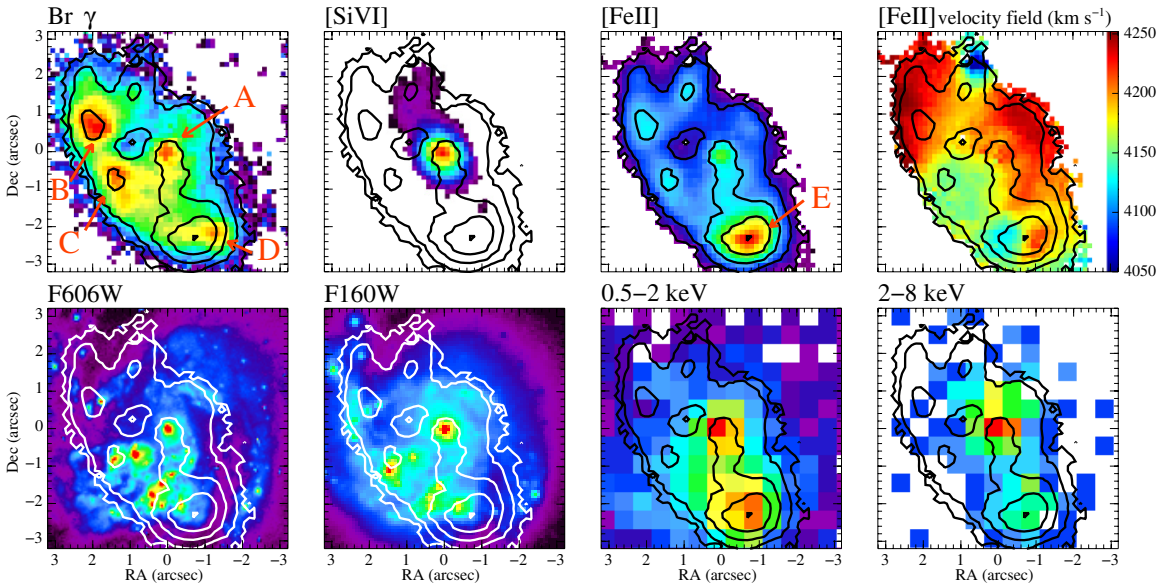

Figure 1. Panel presenting the structure of the central region of NGC 5135 according to different near-IR emission lines (Brγ, [Si VI] 1.96 μm, [Fe II] 1.64 μm), soft (0.5–2 keV), and hard (2–8 keV) X-ray emission, as well as the velocity field of the partially ionized [Fe II] emitting gas. The optical (HST WFPC2 F606W filter) and near-IR (HST NICMOS F160W filter) stellar light distributions are also shown for a direct comparison with the structure of the near-IR and X-ray emitting gas. Individual regions like the nucleus (A) and circumnuclear star-forming regions (B to E) are labeled according to Bedregal et al. (2009). Contours represent the [Fe II] emission distribution. At the assumed distance, 1 arcsec corresponds to 287 pc.

(A color version of this figure is available in the online journal.)

out for local star-forming galaxies such as NGC 253 and M82 (Weaver 2002; Strickland & Heckman 2007), but no adequate data have been available for more powerful starbursts such as LIRGs.

NGC 5135 is a nearby LIRG ($\log(L_{\rm IR}/L_{\odot}) = 11.3$; Pereira-Santaella et al. 2011) with a Compton-thick AGN in its nucleus (Levenson et al. 2004) and several circumnuclear star-forming regions at distances of 1 kpc away from the nucleus, identified by their UV stellar light (Gonzalez-Delgado et al. 1998), (partially) ionized emitting gas (Alonso-Herrero et al. 2006b; Bedregal et al. 2009), and mid-IR 8 μm emission (Alonso-Herrero et al. 2006a). Due to its distance to us (59.2 Mpc), the available near-IR integral field spectroscopy (Bedregal et al. 2009) and X-ray *Chandra* imaging (Levenson et al. 2004) allow us to spatially resolve the structure of its central few kpc region on scales of hundreds of parsecs (1 arcsec corresponds to 287 pc at the assumed distance). The contribution of the different energy sources to the hot X-ray emitting gas and the causal connection between the X-ray emission, in particular hard X-ray, and supernova explosions can therefore be investigated in detail.

2. OBSERVATIONS AND DATA

Near-IR data were obtained with SINFONI, the Very Large Telescope (VLT) near-IR integral field spectrograph. The galaxy was observed in the *H* and *K* bands separately with a spectral resolution of ~3000 and ~4000, respectively. The configuration during the observations was the standard seeing-limited, with a scale of 250 mas per spaxel and a field of view of $8'' \times 8''$. Further details about the calibration process, data reduction, and emission-line measurements can be found elsewhere (Bedregal et al. 2009).

NGC 5135 was observed in X-rays with *Chandra* Advanced CCD Imaging Spectrometer (ACIS) for a total exposure time of 29.3 ks (Levenson et al. 2004). These data have been retrieved from the *Chandra* archive. The `chandra_repro` script (CIAO ver. 4.3) was used to reprocess the level 1 data using the latest available calibration (CALDB ver. 4.4.2). This script performs the recommended data reduction steps[4] (which includes bad pixel removal, corrections for the coordinates and energy of the events, corrections for charge transfer inefficiency, etc.). The local background was measured in a nearby source-free circular region of radius 50 arcsec located 2 arcmin away from the galaxy nucleus. The background light curve was checked to filter out high-background intervals. However, no flares were detected during the observation. Only the events with energies in the interval from 0.3 to 10 keV are considered in the analysis.[5] The spectra of the two bright compact sources (regions A and E in Figure 1) were extracted using a circular aperture of radius 1.5 arcsec. The spectrum of the B+C region was extracted using a 2×3 arcsec elliptical aperture. The response matrix files and the ancillary response files were created assuming a pointlike source. The spectra were grouped to have at least 20 counts in each spectral bin.

3. RESULTS

3.1. Near-IR Emission-line Imaging

The spatially resolved [Fe II] 1.64 μm, Brγ 2.17 μm, and [Si VI] 1.96 μm emission in the central 1.7 kpc by 1.7 kpc region of NGC 5135 is presented together with the soft (0.5–2.0 kV) and hard (2.0–8 keV) X-ray emission in Figure 1. Also given is the velocity field of the interstellar medium (ISM) as traced by the [Fe II] line. The near-IR emission lines and the X-ray continuum trace different phases of the (circum)nuclear ISM, showing clear substructures on scales of hundreds of parsecs and a number of characteristics that trace in detail the

[4] http://cxc.harvard.edu/ciao/threads/data.html

[5] The 0.3–10 keV range is the ACIS-calibrated energy range.

connection between the existing energy sources (AGNs, young stars, shocks) and their impact in the ionization and kinematics of the ISM.

The AGN (region A in Figure 1) is identified as a strong source of coronal [Si VI] emission and appears as a weak Brγ and [Fe II] emitting source. Several Brγ and [Fe II] emitting regions (B to E in Figure 1) trace circumnuclear star-forming clumps at distances of about 1 kpc from the nucleus. While the brightest Brγ region (B in Figure 1) shows a low ($\sim$2) [Fe II] Brγ ratio, the reverse is true for the brightest [Fe II] region (E in Figure 1), where a [Fe II] Brγ ratio of $\sim$20 is measured (Bedregal et al. 2009). These different line ratios can be attributed to a relative age difference of about 4 million years between the star clusters in both regions. Region B would be the youngest ($\leqslant$6 Myr) where massive main-sequence stars are still producing a large number of ionizing photons, e.g., strong hydrogen recombination lines. On the other hand, region E would be more evolved and going through the peak of the supernova phase (i.e., 8–12 Myr), therefore producing locally a strong [Fe II] emission peak, which is spatially coincident with the peak emission at radio wavelengths (see Bedregal et al. 2009 for a discussion on the uncertainties and assumptions). The velocity field of the [Fe II] emission around region E shows locally a velocity gradient along the east–west direction, characterized by a projected peak-to-peak velocity of 90 km s^{-1} and an overall projected size of 300 pc. This structure resembles a biconical outflow with the apex coincident with the peak of the [Fe II] emission (see Figure 1) and is interpreted as a starburst-driven outflow due to the combined effect of several supernovae in region E, consistent with the high supernova explosion rate derived for this region (Bedregal et al. 2009). The morphology of the star-forming regions traced by the ionized gas is consistent with a disk inclined by about 50° with respect to our line of sight. If the axis of the outflow were oriented perpendicular to the plane of the disk, the intrinsic size and outflowing velocities of the [Fe II] emitting gas would be a factor of 1.5–2 higher than the observed values.

3.2. X-ray Imaging

The structure of the X-ray emitting gas is characterized by the presence of two bright soft (0.5–2 keV) and hard (2–8 keV) X-ray unresolved regions, as well as a prominent diffuse emission component in soft X-rays (see Figure 1; and also Levenson et al. 2004). This structure presents interesting features when compared with the near-IR line emitting gas (see Figure 1 and Table 1 for specific luminosities). The brightest soft and hard X-ray emission peaks are associated with the AGN nucleus and therefore coincident with the [Si VI] emission peak. The secondary X-ray emission peak is spatially coincident with the [Fe II] emission peak (region E). Finally, the diffuse soft X-ray emission extends northeast from region E toward region C (secondary extranuclear Brγ peak), avoiding the brightest Brγ emitting region (B in Figure 1) and having an overall structure in surface brightness in better agreement to that shown in [Fe II] emission. Moreover, there also appears to be a kinematic connection between the X-ray and [Fe II] emitting gas as the secondary X-ray peak coincides (within the astrometric uncertainties) with the apex of the biconical [Fe II] outflow. This strongly supports a causal connection between the extremely hot X-ray emitting gas and the supernova explosions in this region of the galaxy (see discussion in Section 4.1).

Table 1
X-Ray and Near-IR Line Luminosities for the Nucleus and Circumnuclear Star-forming Regions of NGC 5135

Region[a]	L(Brγ) (10^{39} erg s^{-1})	L([Fe II]) (10^{39} erg s^{-1})	L(0.5–2 keV) (10^{40} erg s^{-1})	L(2–8 keV) (10^{40} erg s^{-1})
A	0.64	3.65	4.3	13.1
B	0.55	1.17	...	...
C	0.51	1.28	...	...
B+C	1.06	2.45	1.2	<0.5
D	0.35	2.32	...	...
E	0.30	5.50	...	...
D+E	0.65	7.82	6.3	1.4[b]

Notes.
[a] Luminosities for the individual regions (A to E) correspond to apertures with diameters 340 pc (near-IR lines) and 860 pc (X-rays). Regions A to E appear as pointlike. The quoted diameters correspond to the different angular size of the PSF of SINFONI and *Chandra*. Region B+C corresponds to an area of 1.2 kpc × 0.6 kpc as measured in soft X-rays. The X-ray luminosity for regions D and E cannot be measured independently due to the lack of angular resolution in the *Chandra* images.
[b] Detected at 4.5σ level.

4. DISCUSSION

4.1. The X-ray Emission: Origin of the Spatially Resolved Components

As mentioned above, the soft and hard X-ray images show bright nuclear emission (region A in Figure 1), a secondary extranuclear emission coincident with the brightest [Fe II] peak (region E), and a fainter and more diffuse emission, only detectable in soft X-rays, likely associated with the secondary Brγ emission (region C). The physical mechanisms involved in the emission of the X-rays appear to be different in these regions. The X-ray spectrum of the nuclear region has been analyzed in detail by Levenson et al. (2004). They used a model consisting of an absorbed power law, two thermal plasma components, and two Gaussian emission lines at 6.4 and 1.8 kV, respectively. The flat power law ($\Gamma = 0$) and the large equivalent width of the Fe Kα emission line (2.4 keV) indicate that the AGN is highly obscured, with an absorbing column density ($N_{\rm H}$) above 10^{24} cm^{-2}. This conclusion has been recently confirmed by a spectral study of the broad *Suzaku* 0.5–50 keV range, establishing a column density $N_{\rm H}$ of $\sim$2.5 × 10^{24} cm^{-2} toward the AGN (Singh et al. 2012). The spectrum of the B+C region was not explicitly discussed by Levenson et al. (2004). This region is included in their D1 region. Due to the low number of counts of this spectrum (81 counts), Levenson et al. used a simple model with an absorbed power law. The power-law index is 3^{+3}_{-1} and the $N_{\rm H}$ is lower than 5 × 10^{21} cm^{-2}.

Levenson et al. (2004) also discussed the spectrum of the star-forming region identified here as region E. Their model includes a thermal component at 0.7 keV, similar to that found in starbursts (see Persic & Rephaeli 2002), and a power law ($\Gamma = 2.6$). The Fe abundance was allowed to vary to account for the Fe underabundance with respect to α elements observed in star-forming galaxies (e.g., Strickland et al. 2004; Grimes et al. 2005; Iwasawa et al. 2011; Pereira-Santaella et al. 2011). We repeated the analysis and found that this model provides a good fit to the data (χ^2/dof = 34/37; see Table 2). The non-thermal component of the model would be interpreted as emission associated with HMXBs. Although the power law is steeper than individual binary systems, it might be produced by the combination of several individual sources

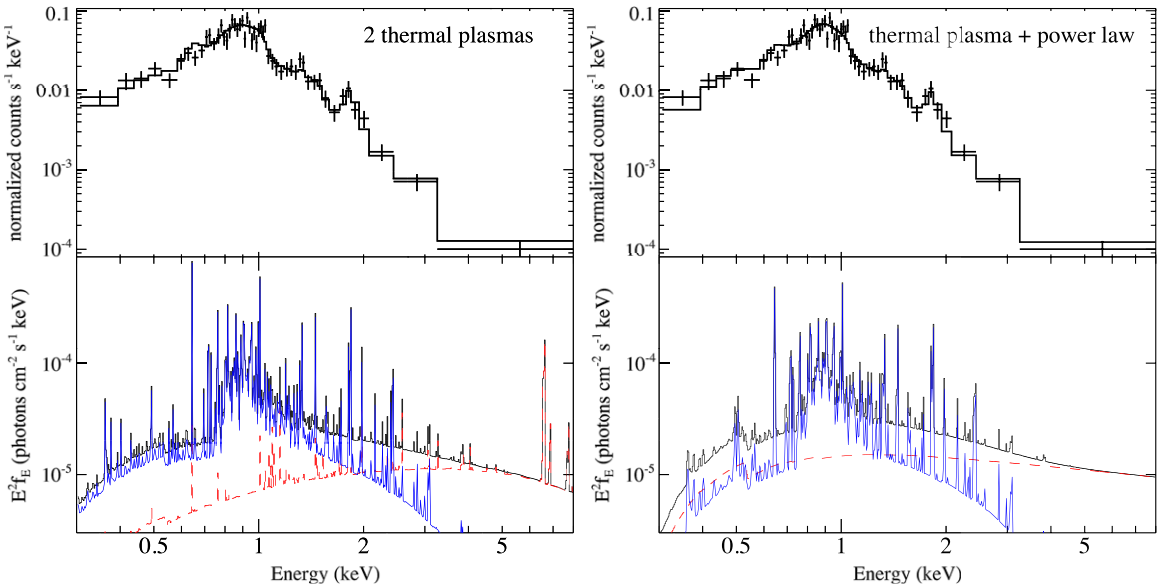

Figure 2. Comparison of the two spectral models for the *Chandra* ACIS spectrum of the region E of NGC 5135 (note that due to lack of angular resolution the spectrum also includes region D identified in the near-IR images). The top panel shows the observed data together with the model (solid black line). The lower panel shows the spectral components of the model: the soft ($kT \sim 0.7$ keV) thermal plasma (solid blue line) and the hard component (hot thermal plasma or power law; dashed red line). The total model is shown in black. The analysis of the X-ray spectral data was done using XSPEC (Arnaud 1996). To account for the Galactic hydrogen column density at the position of NGC 5135 ($N_{\rm H} = 4.9 \times 10^{20}$ cm^{-2}; Kalberla et al. 2005), the TBabs model (Wilms et al. 2000) was adopted.

(A color version of this figure is available in the online journal.)

Table 2
Model Parameters for the Best Fits to the X-ray Spectrum of Region E

Model	$N_{\rm H}$ (10^{20} cm^{-2})	Γ	kT_1 (keV)	Fe/O[a]	kT_2 (keV)	χ^2/dof
Plasma + power law[b]	$8.6^{+5.4}_{-6.0}$	$2.5^{+0.8}_{-0.9}$	$0.68^{+0.07}_{-0.07}$	$0.4^{+0.2}_{-0.1}$	...	34/37
Two plasmas[b]	<10	...	$0.70^{+0.07}_{-0.06}$	$0.3^{+0.1}_{-0.1}$	>2.4	35/37

Notes. The Galactic absorption at the position of NGC 5135 is $N_{\rm H,Gal} = 4.9 \times 10^{20}$ cm^{-2} (Kalberla et al. 2005).
[a] Fe/O abundance ratio with respect to solar values of Anders & Grevesse (1989).
[b] The models used in the fits are Abs($N_{\rm H,Gal}$)*Abs($N_{\rm H}$){power-law(Γ) + vmekal(kT_1, Fe/O)} and Abs($N_{\rm H,Gal}$)*Abs($N_{\rm H}$){vmekal(kT_1, Fe/O) + mekal(kT_2)}, respectively, where Abs is a photoelectric absorption model and (v)mekal is a thermal plasma (with variable Fe abundance).

(Levenson et al. 2004). Alternatively, the spectrum of the region E can be fitted equally well with two thermal components. This model also provides a good fit (χ^2/dof = 35/37; see Table 2). The temperature of the soft thermal component is 0.7 keV, in agreement with previous Levenson et al. (2004) results. Although the hard thermal component is required (with an *F*-test significance >98%), its temperature is not well constrained ($kT > 2.4$ keV). This is due to the low signal-to-noise ratio in the hard X-ray range (only 10 counts are detected above 4 keV in this region). Similar to the nuclear starburst in M82, the soft thermal component would be associated with the extended, diffuse X-ray emitting gas while the hard thermal component would represent extremely hot gas originated in the inner compact region of the starburst directly associated with the strong winds produced by the supernovae (Strickland & Heckman 2007, 2009).

Figure 2 shows the comparison of the two models, while the model parameters and goodness of the fit can be found in Table 2. From the available X-ray spectrum alone both models, as well as both interpretations on the origin of the hard X-ray emission, are plausible. However, the high supernova rate and kinematic evidence of large-scale outflows derived from the SINFONI near-IR data for this region favor the second model, i.e., two thermal gas components, as opposed to the HMXB interpretation (see discussion in following sections).

4.2. Hard X-ray Extranuclear Emission: High-mass X-ray Binaries

As already mentioned in the previous section, the shape of the hard (2–8 keV) X-ray spectrum in region E is also consistent with a power-law energy distribution. This could in principle be explained as due to the contribution of HMXBs. However, arguments based on the absolute hard X-ray luminosity measured in this region do not favor this hypothesis. An entire galaxy like the Milky Way has about 50 HMXBs (Iben et al. 1995) for an estimated SFR of 0.68–1.47 $M_\odot$ yr^{-1} (Robitaille & Whitney 2010), with a mean hard X-ray luminosity of 5×10^{37} erg s^{-1} per HMXB (Persic 2004). So, in order to explain the hard X-ray luminosity 1.4×10^{40} erg s^{-1} emitted by region E, a total of about 280 HMXBs, i.e., close to six times higher than the number of HMXBs in the entire Milky Way, would be required to exist in region E, a small region of less than 400 pc radius (upper limit given by *Chandra* angular resolution). Such a high concentration of low-luminosity HMXBs is very unlikely.

NGC 5135 is an LIRG forming stars at a rate much higher than the Milky Way. It is known that the luminosity function of HMXBs appears to be universal and proportional to

the SFR of the galaxy (Grimm et al. 2003). As a consequence, the luminosity of the brightest HMXB and the number of HMXBs above a certain luminosity increase with the SFR in galaxies. This is empirically supported by the non-detection in the Milky Way of HMXBs with luminosities above 2×10^{38} erg s^{-1} (Grimm et al. 2002) and the detection of several more luminous HMXBs in nearby starburst galaxies. In M82, the closest prototype of a central starburst galaxy, 22 HMXBs with luminosities in the (0.004–3) $\times$ 10^{39} erg s^{-1} range within the central region of 2.5 kpc $\times$ 2.5 kpc have been detected with *Chandra* (Griffiths 2000). Moreover, in the Antennae, a well-known nearby pre-coalescence merger with an infrared luminosity a factor of four lower than that of NGC 5135, a large number of luminous (49) and highly luminous (11 out of 49) HMXBs have been detected with luminosities above 5×10^{37} erg s^{-1} and 10^{39} erg s^{-1}, respectively (Zezas et al. 2002a). These luminous HMXBs are predominantly associated with young stellar clusters, i.e., young stellar populations, and distributed over most of the optical extent of the galaxy (Zezas et al. 2002b), i.e., over a region of about 12 kpc in size. So, even if luminous HMXBs as those detected in M82 and the Antennae exist in NGC 5135, a large number (10–100) of these would be required to be concentrated in a small area in order to explain the hard X-ray luminosity measured in region E. The resulting high density of luminous HMXBs would be orders of magnitude higher than those derived for M82 and the Antennae and unlikely to occur. However, it could still be statistically possible that a single extremely luminous HMXB with a luminosity close to the cutoff (2×10^{40} erg s^{-1}) of the luminosity function would exist in NGC 5135 and be located in region E. Highly variable ultraluminous X-ray sources have recently been detected in NGC 1365 (Strateva & Komossa 2009) and even in M82 (M82 X1; Voss et al. 2011). If this were the case, a measurable variability of the X-ray emission in this region would be expected (Gilfanov et al. 2004). A monitoring of NGC 5135 with *Chandra* would be needed to confirm or reject this scenario.

4.3. Hard X-ray Extranuclear Emission: Supernova-driven Hot Outflowing Winds

Detailed X-ray imaging of M82 has shown that the structure of the hard X-ray diffuse emission is similar to that of the nuclear starburst, as traced by the spatial distribution of the compact radio sources, most of which are young supernova remnants (Strickland & Heckman 2007). Moreover, the extent of the hard X-ray diffuse emission is much smaller than the overall size of the diffuse soft X-ray emission that extends above and below the plane of the galaxy, i.e., minor axis, up to distances of 5–6 kpc (Strickland & Heckman 2007, 2009, and references therein). This has been interpreted as the unambiguous sign of young massive stars and their associated supernova-driven winds as the direct origin of the diffuse hard X-ray emission. Similarly in NGC 5135, the spatial coincidence of the peak of the [Fe II] emission, the apex of the [Fe II] outflow, and the secondary X-ray emission peak favors a common physical origin for these emissions. The [Fe II] emission with its associated outflow has its natural explanation as the combined effect of supernova explosions in this region of the galaxy. Bedregal et al. (2009) derived a supernova rate of 0.05–0.1 yr^{-1} for region E using the radio and [Fe II] luminosities and various empirical and model calibrations (see references in Bedregal et al. 2009). Since each supernova releases a total of 10^{51} erg in kinetic energy (Chevalier 1977), the expected energy release for the estimated supernova rate amounts to (1.6–3.2) $\times$ 10^{42} erg s^{-1}. This value agrees remarkably well with the predicted mechanical energy in shocks derived from the [Fe II] luminosity. Assuming an [Fe II] 1.257 μm/[Fe II] 1.644 μm line ratio of 1.36 (Nussbaumer & Storey, 1988) and typical [Fe II] 1.257 μm luminosity to shock energy ratios of (3–5) $\times$ 10^{-3} for velocity shocks of 75–150 km s^{-1} (Mouri et al. 2000), a total energy in shocks equal to 2.7×10^{42} erg s^{-1} is obtained.

An additional estimate of the mechanical energy can also be derived directly from the outflowing velocity and the shocked gas mass associated with the [Fe II] emission. The overall kinetic energy is given as $0.5 \times M^{\rm gas}_{\rm shocks} \times V^2_{\rm outflow}$, where the mass of gas is directly proportional to the [Fe II] luminosity and inversely proportional to the particle density of the gas. Assuming solar abundances, an [Fe II] emissivity per unit of volume of (1.3–1.6) $\times$ 10^{-20} erg cm^3 s^{-1} (Mouri et al. 2000), particle densities of about 10^3 cm^{-3} (i.e., well below the critical density of the [Fe II] lines), and intrinsic outflowing velocities of about 100 km s^{-1}, the derived kinetic energy is $\sim$1 $\times$ 10^{52} erg. This would be equivalent to the combined kinetic energy release of between 10 and 100 supernovae for a high to moderate thermalization efficiency, respectively.

The strong [Fe II] emitting region (E in Figure 1), although spatially resolved in the VLT/SINFONI observations, is compact with an upper limit to its effective (i.e., half-light) radius (R_e) of 80 pc. Therefore, the [Fe II] emission detected in this region is consistent with the combined effect of a large number of supernovae confined in a small volume. A high number of supernovae have also been identified at radio frequencies in the nuclear region (150 pc in size) of Arp299A (IC 694), a well-known LIRG (Perez-Torres et al. 2009; Bondi et al. 2012). Under these conditions, models developed to explain the diffuse hard X-ray emission in M82 (Strickland & Heckman 2009) predict that an important fraction of the kinetic energy released by the supernovae will actually drive bulk motions of the surrounding interstellar gas, i.e., will have a high thermalization efficiency. As a consequence, the surrounding ISM will increase its temperature to tens to hundreds of million kelvin, emitting not only soft but also hard X-rays. In these models, for a given thermalization efficiency (ϵ) and mass loading factor (β), the hard X-ray luminosity is inversely proportional to the size of the region ($L_{\rm HX} \propto \epsilon^{-1} \times \beta^3 \times R_e^{-1}$; see Equations (8) and (16) in Strickland & Heckman 2009). A 10 Myr old instantaneous burst releasing a total (supernova and massive stars) mechanical energy of 4.5×10^{42} erg s^{-1} with a high thermalization efficiency ($\epsilon = 1.0$) and no mass loading ($\beta = 1.0$) in a region of 285 pc radius would produce a hard X-ray luminosity of 5×10^{38} erg s^{-1} (model C; Strickland & Heckman 2009). Scaling linearly with the effective radius of the [Fe II] emitting region ($R_e \leqslant 80$ pc), the expected hard X-ray luminosity for region E would be about 2×10^{39} erg s^{-1}, a factor of seven less than measured (see Table 1). This predicted HX is, however, a lower limit. It could largely increase if the thermalization efficiency were lower than 1 and, in particular, if the mass loading factor, which represents the contribution to the total mass swept by the wind due to the cold ambient ISM, were larger than 1 ($L_{\rm HX} \propto \beta^3$). The measured properties of the diffuse hard X-ray emission in M82 are compatible with a range of models characterized by thermalization efficiencies between 0.3 and 1.0 and mass loading factors between 1.0 and 2.8 (Strickland & Heckman 2009). In the highly active star-forming and dense molecular gas environments of the central regions of LIRGs, similar conditions as those in M82 are likely to be present. Therefore, the measured hard X-ray luminosity in NGC 5135 would be consistent with the

predictions for a mass loading factor and thermalization efficiency of 2.5 and 0.5, respectively. In addition, the total luminosity predicted by the models as due to the hot thermalized medium is about 2.5 times higher than its hard X-ray luminosity (see Table 7 of Strickland & Heckman 2009), i.e., close to the 4.5 factor measured for the soft to hard X-ray emission ratio in region E.

4.4. Hard X-ray Emission and Star Formation Rates

As in many other wavelengths (UV, Hα, infrared, radio), the X-ray luminosity has also been used as a tracer of the star formation in starburst galaxies. Empirical linear relations have been established between soft and hard X-ray luminosities and SFRs, under the assumption of constant star formation (e.g., Pereira-Santaella et al. 2011, and references therein). These relations are obtained using the observed infrared continuum and optical recombination line luminosities as direct tracers of the obscured and unobscured SFRs. It is also generally accepted that in the absence of an AGN, the hard X-ray emission in galaxies is due to low- and high-mass X-ray binaries (LMXBs and HMXBs, respectively), with HMXBs dominating the hard X-ray emission in extreme starbursts such as non-AGN LIRGs and ULIRGs (Persic & Rephaeli 2002; Grimm et al. 2003; Lehmer et al. 2010).

Although these relations appear to hold for starbursts covering a wide range of SFRs, they show a factor of four peak-to-peak scatter (1σ) around the best fit (e.g., Pereira-Santaella et al. 2011). This scatter is likely to have a real physical origin and is worth discussing further. On the one hand, the empirical data used to derive the obscured (i.e., infrared bright) and unobscured (i.e., UV or optical bright) star formation lacks usually the appropriate spatial resolution and assumes implicitly that these regions also emit hard X-rays. This is clearly not the case for NGC 5135, where, outside the nucleus, the dominant Paα (Alonso-Herrero et al. 2006b) and Brγ (Figure 1) emission peaks correspond to a circumnuclear region that is spatially independent from the dominant hard X-ray emitting region and located at a distance of about 1.2 kpc from it. Moreover, subarcsec mid-IR imaging (Alonso-Herrero et al. 2006a) shows that the mid-IR emission outside the AGN is distributed in four almost equally bright regions, the Brγ and hard X-ray peaks and two other regions at distances of about 1 kpc from the hard X-ray emitting peak. On the other hand, the assumption that the X-ray emission is dominated by the contribution of compact sources associated with LMXBs and HMXBs is not necessarily realistic. Evidence for the presence of diffuse, extended soft and hard X-ray emitting regions has now been firmly established in the nuclear starburst region of nearby galaxies like NGC 253 (Weaver 2002; Mitsuishi et al. 2011) and M82 (Strickland & Heckman 2007), although with different physical origins. The hard X-ray emission in NGC 253 appears to be not only due to photoionization by a low-luminosity AGN (Weaver 2002) but also associated with the combined energy output of tens to hundreds of supernovae (Mitsuishi et al. 2011). The extent of the hard X-ray emission in M82 is similar to the distribution of the radio sources (e.g., young supernova remnants). Therefore, it is likely that in NGC 253 and M82 there is a relation between supernova explosions, and subsequent winds, and the diffuse hard X-ray emitting gas (Strickland & Heckman 2007). As already mentioned (Section 4.3), detailed modeling of the supernova-related superwinds predicts the generation of diffuse hard X-ray emitting plasma in compact and highly thermalized starburst regions (Strickland & Heckman 2009).

Taking M82 as a prototype of a low-luminosity starburst (i.e., $L_{\rm IR} < 10^{11}\ L_{\odot}$), the diffuse component is responsible for most (90%) of its soft X-ray emission in the nuclear region (0.5 kpc radius). In hard X-rays, while the dominant contribution is due to point sources likely associated with binaries (Strickland & Heckman 2007), the diffuse component makes a relevant contribution (∼20%–30%) to the total hard X-ray emission (see Table 2 of Strickland & Heckman 2007). Moreover, recent X-ray studies of a large sample of LIRGs and ULIRGs ($\log L_{\rm IR}$= 11.73–12.57 $L_{\odot}$) show in non-AGN sources an X-ray excess compatible with strong Fe XXV emission at 6.7 keV (Iwasawa et al. 2009). The presence of this high-ionization Fe line is incompatible with HMXB emission, and it is likely due to a high-temperature ($T \sim 10^8$ K) plasma (Iwasawa et al. 2009). These authors also conclude that unlike for local star-forming galaxies, HMXBs are not the primary source of the hard X-ray emission seen in these non-AGN (U)LIRGs, suggesting that a transition in the nature of the dominant hard X-ray source from massive X-ray binaries to hot diffuse plasma occurs somewhere in the range $\log (L_{\rm IR}/L_{\odot})$= 11.0–11.73 (Iwasawa et al. 2011). Moreover, recent X-ray studies of the nuclear region of NGC 253 reinforce this scenario. These studies (Mitsuishi et al. 2011) demonstrate that the FeK line complex emission is extended and distributed in a 60 arcsec^2 region around the nucleus, with the highly ionized lines explained by the cumulative emission of hundreds of supernovae with a minor contribution from binaries.

NGC 5135 with an infrared luminosity ($L_{\rm IR}$) of $2 \times 10^{11}\ L_{\odot}$ can be considered as a prototype of LIRGs that happens to be close enough for a detailed investigation of the spatial distribution and physical origin of the hard X-ray emission. As already shown (see Section 3), the hard X-ray luminosity is dominated (82%) by the AGN, while the rest is associated with the [Fe II] peak (9%) and regions confined within 1 kpc around it (9%). So, aside from the AGN contribution, the hard X-ray emission in NGC 5135 is due to supernova-driven hot plasma confined in small regions. This physical scenario could also be present in an important fraction of non-AGN LIRGs and ULIRGs. The overall size of the starburst region in LIRGs traced by near-IR and optical hydrogen lines (Alonso-Herrero et al. 2006a; Rodriguez-Zaurin 2011) or mid-IR continuum emission is typically a few kpc, distributed in few to several high surface brightness clumps of hundreds of pc each. Our ongoing SINFONI survey (Piqueras et al. 2012) shows that many nearby LIRGs have few to several bright compact [Fe II] emitting regions in their (circum)nuclear regions. Moreover, some of these LIRGs (NGC 3256 and IC 694) do show in their integrated X-ray spectrum highly ionized iron Kα emission lines (Pereira-Santaella et al. 2011; Ballo et al. 2004), supporting therefore the hypothesis that an important, if not dominant, fraction of the hard X-rays in these galaxies is associated with hot plasma emission.

If the hard X-ray emission in non-AGN U/LIRGs is not dominated by the HMXB emission but rather by a supernova-driven hot X-ray emitting plasma, the meaning of the SFRs derived from the hard X-ray luminosity has to be reconsidered. The X-ray emission of HMXBs and hot plasma are due to different physical mechanisms, accretion versus thermalized hot plasma, and subject to different physical parameters. In fact, while the number of luminous HMXBs appears to scale linearly with the SFR (Persic 2004), the hot X-ray emitting gas shows a nonlinear relation with the SFR according to models ($L_{\rm HX} \propto {\rm SFR}^2$; Strickland & Heckman 2009). Moreover, while both supernovae and HMXBs are associated with

massive stars, their birthrate and life span differ significantly (Persic & Rephaeli 2002; Iben et al. 1995), and therefore the associated SFR would also be different. An indication that this could be the case is given by the discrepancy in the derived SFR values for NGC 5135 when calculated using the different empirical relations based on the 24 μm, soft and hard X-ray luminosities (see Pereira-Santaella et al. 2011 for specific relations). NGC 5135 has an AGN, and therefore corrections to its contribution to the luminosity of the galaxy have to be applied before calculating SFRs. The AGN contribution to the 24 μm luminosity was derived from the decomposition of the Spitzer Infrared Spectrograph low-resolution 5–38 m spectrum into AGN and starburst components using clumpy torus models and star-forming galaxy templates (Alonso-Herrero et al. 2012). The AGN soft and hard X-ray luminosities were derived directly from the *Chandra* images (see Table 1 for specific values) and subtracted from the integrated X-ray emission. Correcting for the AGN as above, the total SFR of the central 2 kpc starburst derived from the hard X-ray luminosity gives a lower limit with a factor of two and four lower than that obtained from the infrared and soft X-ray luminosities, respectively. A plausible explanation for this discrepancy is that the regions dominating the integrated emission at different wavelengths appear at different locations within the galaxy and separated by hundreds of pc, i.e., different physical origin, different evolutionary phases, and no causal connection between the regions. This is the case for NGC 5135, where, aside from the AGN, the hard X-ray emission appears to be dominated (>50%) by region E, the soft X-rays show a more extended emission with contributions from region E, as well as other compact regions and diffuse emission (Figure 1; Levenson et al. 2004), and the mid-IR emission is distributed in several circumnuclear star-forming regions located at distances of about 1–1.2 kpc from region E (Alonso-Herrero et al. 2006a). This is in agreement with a scenario where for a given LIRG the hard X-rays would be produced mainly in a subset of star-forming regions characterized by its compactness (i.e., less than hundred parsecs), very high SFR densities ($L_{\rm HX} \propto {\rm SFR}^2/R$; according to Strickland & Heckman 2009 models), and a large supernova rate, while the soft X-rays and IR emission would trace the young massive stars associated with the overall star formation in larger (kpc size) regions. Under this scenario, the hard X-ray emission would give a lower limit to the SFR, as is the case in NGC 5135. This scenario would also give a natural explanation, other than the absorption effects, to the deficit of hard X-ray emission measured in LIRGs and ULIRGs with respect to the values expected from their IR-derived SFRs (Lehmer et al. 2010).

High angular X-ray and [Fe II] imaging of a large sample of nearby LIRGs is needed in order to further investigate the origin and quantify the contribution of starburst-driven hot ISM to the hard X-ray emission in LIRGs and therefore validate the use of hard X-ray luminosity to derive accurate estimates of star-forming rates in these galaxies.

5. CONCLUSIONS

Near-infrared integral field spectroscopy of the LIRG NGC 5135 combined with archival high-resolution *Chandra* X-ray imaging has been used to investigate in detail the physical origin of its hard X-ray emission and to establish the validity of the hypothesis behind the SFRs derived from the hard X-ray luminosities in LIRGs and ULIRGs. The main conclusions are as follows:

1. The AGN is identified in the near-IR by a strong [Si VI] 1.96 μm emission showing a nuclear component and an extended diffuse elongation of about 0.6 kpc toward the north of the nucleus. The AGN generates 90% of the hard X-ray luminosity emitted within the central 2 kpc diameter. There are hints of a connection between the diffuse [Si VI] emitting gas and the hard X-ray emission north of the AGN.
2. The strongest [Fe II] emission peak (region E) is located at a distance of about 0.9 kpc southwest of the AGN showing a local velocity field with the kinematical characteristics of outflowing material. The [Fe II] luminosity and kinetic energy in this region are consistent with the scenario of supernova-induced outflows and with previous estimates of the supernova rate (0.05–0.1 SNe yr^{-1}) in this region.
3. The luminous hard X-ray emitting region outside the AGN coincides with the strongest [Fe II] peak and associated outflowing material. A direct causal connection appears to exist between supernova-induced winds and shocks and the hard X-ray emitting ISM in this region. This result is in agreement with recent scenarios where starbursts confined in small volumes and with high thermalization efficiencies are able to heat the ISM to temperatures of 10–100 million degrees, emitting therefore hard X-rays. Starbursts in U/LIRGs are compact and confined to small regions, and therefore the hot diffuse X-ray emitting gas could represent an important (even dominant) contribution to the overall hard X-ray emission.
4. The alternative explanation of the hard X-ray emission outside the AGN as due to HMXBs is not favored although cannot be ruled out. If luminous HMXBs similar to those detected in other nearby starburst galaxies like M82 and the Antennae exist in NGC 5135, a much higher density of HMXBs (>10–100 pc^{-2}) would be required to explain the hard X-ray luminosity in region E. The possibility of having a single, extremely luminous HMXB with a luminosity close to the cutoff limit ($L_{\rm HX} = 2 \times 10^{40}$ erg s^{-1}) of the HMXB luminosity function is still compatible with the measured luminosity.
5. The SFR in NGC 5135 derived from the hard X-ray luminosity gives a lower limit corresponding to factors two and four lower than the 24 μm and soft X-ray-derived values, respectively. This is understood as a consequence of the contribution of the different star-forming regions. The dominant mid-IR (and Brγ) emitting regions are spatially separated by distances of about 1 kpc from the extended soft and compact hard X-ray emitting regions. Thus, the individual star-forming regions are physically disconnected and appear to be in different evolutionary states (i.e., age, ISM), contributing differently to the emission at various wavelengths.
6. The origin and nature of the hard X-ray emission in LIRGs like NGC 5135 have to be investigated in more detail through high angular resolution X-ray, complemented with near- and mid-infrared imaging, in a larger sample of galaxies. If, according to the models and the evidence shown so far in NGC 5135, the hard X-ray emission traces the more compact star-forming regions with the highest star-forming densities ($L_{\rm HX} \propto {\rm SFR}^2/R$), the hard X-ray emission in these galaxies would appear associated with compact, luminous [Fe II] emitting star-forming regions and would represent a lower limit to the overall SFR, traced by the more extended IR and soft X-ray emission.

M.P.-S. acknowledges support from CSIC under grant JAE-Predoc-2007. This work has been supported by the Spanish Plan Nacional del Espacio under grants ESP2007-65475-C02-01 and AYA2010-21161-C02-01.

REFERENCES

Alonso-Herrero, A., Colina, L., Packham, C., et al. 2006a, ApJ, 652, L83
Alonso-Herrero, A., Pereira-Santaella, M., Rieke, G. H., & Rigopoulou, D. 2012, ApJ, 744, 2
Alonso-Herrero, A., Rieke, G. H., Rieke, M. J., et al. 2006b, ApJ, 650, 835
Anders, E., & Grevesse, N. 1989, Geochim. Cosmochim. Acta, 53, 197
Arnaud, K. A. 1996, in ASP Conf. Ser. 101, Astronomical Data Analysis Software and Systems V, ed. G. H. Jacoby & J. Barnes (San Francisco, CA: ASP), 17
Ballo, L., Braito, V., Della Ceca, R., et al. 2004, ApJ, 600, 634
Bedregal, A., Colina, L., Alonso-Herrero, A., & Arribas, S. 2009, ApJ, 698, 1852
Bondi, M., Perez-Torres, M. A., Herrero-Illana, R., & Alberdi, A. 2012, A&A, in press (arXiv:1201.3220)
Chevalier, R. A. 1977, ARA&A, 15, 175
Genzel, R., Lutz, D., Sturm, E., et al. 1998, ApJ, 498, 579
Gilfanov, M., Grimm, H. J., & Sunyaev, R. 2004, MNRAS, 351, 1365
Gonzalez-Delgado, R., Heckman, T., Leitherer, C., et al. 1998, ApJ, 505, 174
Griffiths, R. E., Ptak, A., Feigelson, E. D., et al. 2000, Science, 290, 1325
Grimes, J. P., Heckman, T., Strickland, D., & Ptak, A. 2005, ApJ, 628, 187
Grimm, H. J., Gilfanov, M., & Sunyaef, R. 2002, A&A, 391, 923
Grimm, H. J., Gilfanov, M., & Sunyaef, R. 2003, MNRAS, 339, 793
Iben, I., Tutukov, A. V., & Yungelson, L. R. 1995, ApJS, 100, 217
Iwasawa, K., Sanders, D. B., Evans, A. S., et al. 2009, ApJ, 695, L103
Iwasawa, K., Sanders, D. B., Teng, S. H., et al. 2011, A&A, 529, 106
Kalberla, P. M. W., Burton, W. B., Hartmann, D., et al. 2005, A&A, 440, 775
Lehmer, B. D., Alexander, D. M., Bauer, F. E., et al. 2010, ApJ, 724, 559
Levenson, N. A., Weaver, K. A., Heckman, T. M., Awaki, H., & Terashima, Y. 2004, ApJ, 602, 135
McDowell, J. C., Clements, D. L., Lamb, S. A., et al. 2003, ApJ, 591, 154
Mitsuishi, I., Yanasaki, N. Y., & Takei, Y. 2011, ApJ, 742, L31
Mouri, H., Kawara, K., & Taniguchi, Y. 2000, ApJ, 528, 186
Nandra, K., O'Neill, P. M., George, I. M., & Reeves, J. N. 2007, MNRAS, 382, 194
Nardini, E., Risaliti, G., Salvati, M., et al. 2008, MNRAS, 385, L130
Nussbaumer, H., & Storey, P. J. 1988, A&A, 193, 327
Pereira-Santaella, M., Alonso-Herrero, A., Santos-Lleo, M., et al. 2011, A&A, 535, A93
Perez-Torres, M., Romero-Cañizales, C., Alberdi, A., & Polatidis, A. 2009, A&A, 507, L17
Persic, M., Cappi, M., Raphaeli, Y., et al. 2004, A&A, 419, 849
Persic, M., & Rephaeli, Y. 2002, A&A, 382, 843
Piqueras, J., Colina, L., Arribas, S., et al. 2012, A&A, submitted
Ranalli, P., Comastri, A., & Setti, G. 2003, A&A, 399, 39
Robitaille, T. P., & Whitney, B. A. 2010, ApJ, 710, L11
Rodriguez-Zaurin, J., Arribas, S., Monreal-Ibero, A., et al. 2011, A&A, 527, 60
Singh, V., Risaliti, G., Braito, V., & Shastri, P. 2012, MNRAS, 419, 2089
Strateva, I. K., & Komossa, S. 2009, ApJ, 692, 443
Strickland, D., & Heckman, T. M. 2007, ApJ, 658, 258
Strickland, D., & Heckman, T. M. 2009, ApJ, 697, 2030
Strickland, D., Heckman, T. M., Colbert, E. J. M., Hoopes, C. G., & Weaver, K. A. 2004, ApJS, 151, 193
Strickland, D., Heckman, T. M., Weaver, K. A., Hoopes, C. G., & Dahlem, M. 2002, ApJ, 568, 689
Voss, R., Nielsen, M. T. B., Nelemans, G., Fraser, M., & Smartt, S. J. 2011, MNRAS, 418, L124
Weaver, K. A., Heckman, T. M., Strickland, D. K., & Dahlem, M. 2002, ApJ, 576, L19
Wilms, J., Allen, A., & McCray, R. 2000, ApJ, 542, 914
Zezas, A., Fabbiano, G., Rots, A. H., & Murray, S. S. 2002a, ApJS, 142, 239
Zezas, A., Fabbiano, G., Rots, A. H., & Murray, S. S. 2002b, ApJ, 577, 710